Mixing Time Optimization of Chitosan-Bentonite Composites for Sustainable Clay Liner Applications

Yulian Firmana Arifin
Civil Engineering Study Program, University of Lambung Mangkurat, Banjarbaru, Indonesia | Wetland-Based Material Research Center, University of Lambung Mangkurat, Banjarbaru, Indonesia
y.arifin@ulm.ac.id (corresponding author)

Rusdiansyah Rusdiansyah
Civil Engineering Study Program, University of Lambung Mangkurat, Banjarbaru, Indonesia
rusdiansyah74@ulm.ac.id

Adriani Adriani
Civil Engineering Study Program, University of Lambung Mangkurat, Banjarbaru, Indonesia
adriani.sipil@ulm.ac.id

Muhammad Nur Arfiandoyo
Civil Engineering Study Program, University of Lambung Mangkurat, Banjarbaru, Indonesia
arfiandoyo@gmail.com

Muhammad Naufal Herfian Rizqullah
Civil Engineering Study Program, University of Lambung Mangkurat, Banjarbaru, Indonesia
naufalherfian19@gmail.com

Received: 28 December 2024 | Revised: 26 January 2025 | Accepted: 29 January 2025

 DOI: https://doi.org/10.48084/etasr.10062

ABSTRACT

Bentonite-chitosan composites offer promising potential as clay liners due to their low permeability and enhanced mechanical properties. However, the extended mixing times required for optimal composite performance pose challenges for large-scale applications. This study investigates the effects of varying mixing times on the properties of bentonite-chitosan composites to optimize their performance while improving practicality. The composites were prepared by mixing bentonite with chitosan in acetic acid and sodium tripolyphosphate (STPP) solutions for varying durations. Characterization tests, including FTIR, TGA, and SEM-EDX, were conducted to assess the chemical interactions, thermal stability, and morphology. The plasticity was evaluated through the Liquid Limit (LL) and Plasticity Index (PI), while the permeability was tested using the falling head method at 16 kN/m³ density and 10% water content. The results indicated that longer mixing times, particularly 2 hours in acetic acid and 4 hours in STPP, resulted in the lowest permeability (1×10^{-12} m/s) and the best structural integrity. However, shorter mixing times, such as 2 hours in acetic acid and 2 hours in STPP, also provided acceptable performance, offering a practical alternative. Pure bentonite, while exhibiting low permeability, lacked the structural integrity achieved by chitosan-enhanced composites. Future research should focus on evaluating the long-term durability of these composites under field conditions, their scalability, and performance in sand-bentonite mixtures, emphasizing the role of optimized mixing times in improving composite performance.

Keywords-bentonite-chitosan composite; acetic acid; sodium tripolyphosphate; permeability; clay liner

I. INTRODUCTION

Chitosan, a natural linear polysaccharide derived from chitin, has gained significant attention across various fields due to its unique properties. As an environmentally friendly and biodegradable polymer, it is widely used in material science [1]. In the construction sector, chitosan is often combined with other materials, such as clay, to enhance its properties. Its non-

hygroscopic nature and electrostatic interactions with negatively charged clay improve the composite's characteristics, making it suitable as a barrier material [2, 3]. This principle underlies the application of chitosan in bentonite-chitosan mixtures, particularly for use as barrier materials in landfill clay liners. Studies have shown that adding chitosan, at concentrations ranging from 2% to 6% by weight of bentonite, significantly enhances plasticity, reduces permeability, and increases the compressive strength of the mixture [4]. Additionally, incorporating chitosan into bentonite-based bio nanocomposites has been found to lower permeability to levels that meet the required thresholds for clay liners at specific sand contents [5].

Despite these advantages, the preparation of bentonite-chitosan composites remains highly time-intensive, typically requiring six hours: two hours of mixing with a 2% acetic acid solution followed by four hours with a 5 wt% STPP solution [4-6]. This prolonged mixing duration poses challenges to scalability and efficiency. Furthermore, existing research has yet to fully explore the optimization of key mixing parameters, such as mixing time, initial chitosan concentration, chitosan-to-clay ratio, and clay type [7, 8]. Given the critical need for time-efficient material synthesis, it is essential to investigate methods that reduce the mixing duration without compromising the composite's performance -particularly in achieving permeability values below 1×10^{-9} m/s.

To address these challenges, this study builds upon previous methodologies [4-6], focusing on optimizing the mixing process. By maintaining consistent concentrations of the mixing solutions, the study aims to reduce the duration of each stage while ensuring that the resultant composite meets the required permeability of 1×10^{-9} m/s. Characterization techniques -including Fourier-Transform Infrared Spectroscopy (FTIR), X-Ray Diffraction (XRD), X-Ray Fluorescence (XRF), Thermogravimetric Analysis (TGA), and Scanning Electron Microscopy (SEM)- are employed to analyze the composite's chemical properties, crystalline structure, elemental composition, and microstructural morphology. Existing studies have explored various aspects of chitosan-bentonite composites. For instance, bentonite, commonly used in clay liners, requires an optimal mix ratio with sand to control its expansive nature and permeability [9]. While synthetic polymers have been used to reduce the required bentonite content, natural polymers, like chitosan, offer a more sustainable alternative [6, 10-12]. Prior research has demonstrated that bentonite-chitosan mixtures can achieve low permeability at specific chitosan concentrations (2%, 4%, and 6%) [4]. However, the impact of prolonged mixing times (six hours) on efficiency and scalability has not been thoroughly investigated [6]. Additionally, the preparation stages, dissolving chitosan in acetic acid [4, 5, 13-17] and reinforcing the mixture with STPP for colloidal stability [4, 5, 11, 18-21] have been conducted independently in various studies, leaving a gap in understanding how to optimize the overall mixing time. This study aims to bridge these gaps by systematically reducing the mixing duration and evaluating its effect on composite performance.

The primary objective of this research is to minimize the mixing time of bentonite and chitosan while ensuring that the composite meets the permeability requirements for clay liners. The novelty of this study lies in its systematic approach to reducing the total preparation time by analyzing the efficiency of each mixing stage. This work contributes to the development of more efficient and sustainable construction materials, particularly for landfill applications, by providing a scientific basis for time-optimized synthesis processes.

II. MATERIALS AND METHODS

A. Bentonite

The bentonite utilized in this study was commercial sourced from Indonesia and is characterized by its high clay content and unique physical and chemical properties. It has a specific gravity of 2.71 and a natural water content of 11%. The soil composition primarily consists of clay (54.81%) and silt (40.38%), with a minor fraction of fine sand (4.81%). Bentonite exhibits exceptional plasticity, with an LL of 371.45, a Plastic Limit (PL) of 42.43, and a PI of 329.02. These high plasticity values indicate its excellent ability to deform under stress without cracking, making it ideal for applications requiring impermeable barriers. Additionally, its Cation Exchange Capacity (CEC) of 52.20 meq/100 g of dry soil highlights its strong ion-exchange capability, which is crucial for enhancing interactions with other materials, such as polymers. These properties confirm the suitability of this bentonite for use in clay liner applications. The XRF analysis of the bentonite sample revealed that its dominant components are silicon (Si, 41.5%), aluminum (Al, 11%), and iron (Fe, 37.2%), confirming its composition as an aluminosilicate, primarily montmorillonite. Additionally, calcium (Ca, 5.61%) represents exchangeable cations, which play a key role in swelling and ion-exchange properties. These results further validate the bentonite's suitability for clay liner applications due to its high Si-Al content and CEC. Figure 1 illustrates the XRD pattern and peak characteristics of bentonite. The XRD analysis identifies key peaks at $2\theta=19.79^{o}$ (d-spacing = 4.49 Å), 21.92^{o} (d-spacing = 4.05 Å), and 24.27^{o} (d-spacing = 3.67 Å) with relative intensities of 27.01%, 16.64%, and 100%, respectively. These peaks correspond to montmorillonite, the main mineral in bentonite. A peak at $2\theta=26.64^{o}$ (d-spacing = 3.35 Å, 23.20% relative intensity) represents quartz, a common impurity. Lower-intensity peaks at $2\theta=35.08^{o}$, 50.07^{o}, and 61.87^{o}, with d-spacings of 2.56 Å, 1.82 Å, and 1.50 Å, respectively, the presence of minor phases, such as feldspar. These findings confirm montmorillonite's dominance, supporting its suitability for clay liner applications due to its swelling capacity and low permeability.

B. Chitosan

The chitosan utilized in this research was derived from crab and shrimp shells and processed into a fine powder with a particle size ranging between Mesh 100 and 300. It has a degree of deacetylation of 87.5%, indicating a high level of purity and a substantial presence of functional amine groups. These characteristics make it highly reactive and suitable for adsorption processes and composite material development.

The FTIR spectrum of the chitosan sample confirms its molecular structure through key absorption bands, as illustrated in Figure 2. The broad peak observed between 3,420-3,300 cm^{-1} corresponds to O-H and N-H stretching, indicating the presence of hydroxyl and amine groups. The peak at 2,920 cm^{-1} is attributed to C-H stretching in the polysaccharide backbone. The strong absorption bands at 1,650 cm^{-1} and 1,560 cm^{-1} are associated with amide I (C=O stretching) and amide II (N-H bending and C-N stretching), confirming partial deacetylation. Additionally the peaks at 1,400 cm^{-1} (C-H bending), 1,030–1,150 cm^{-1} (C-O-C stretching), and 897 cm^{-1} (β-glycosidic linkages) further validate its polymeric structure. These functional groups confirm chitosan's suitability for composite applications.

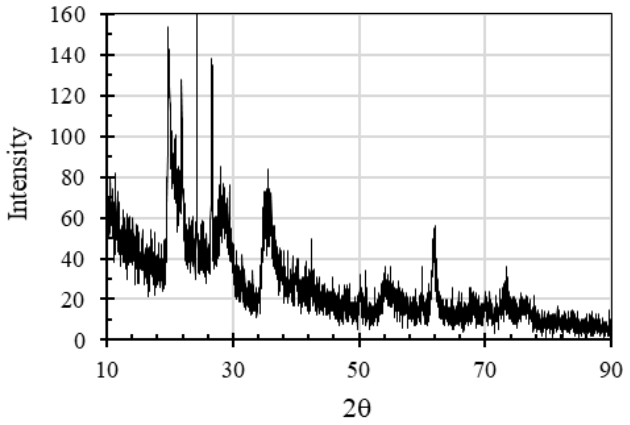

Fig. 1. XRD pattern and peak charcteristics of bentonite.

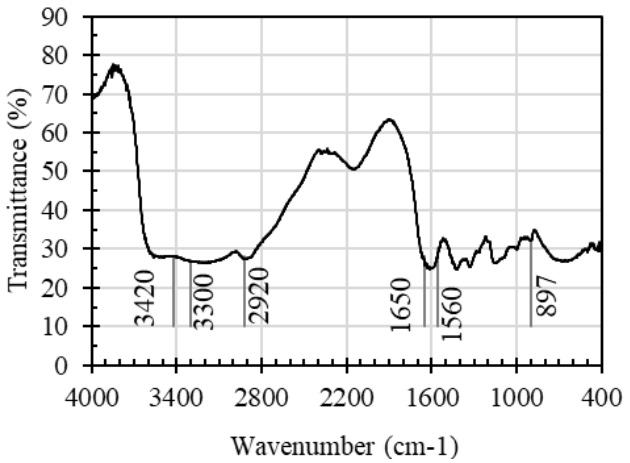

Fig. 2. FTIR spectrum of chitosan presenting characteristic functional groups.

C. Sample Preparation

The mixing process of chitosan and bentonite followed the procedures established by several researchers [6, 22], as later adapted in [4], to determine the optimal composition of 2% chitosan and 98% bentonite. The preparation process for the 2% chitosan composition involved several sequential steps:

- Preparation of Acetic Acid Solution: A 2% (v/v) acetic acid solution was prepared.
- Dissolution of Chitosan: 2 g of powdered chitosan was added to the acetic acid solution and mixed at 60°C until fully dissolved.
- Incorporation of Bentonite: 98 g of bentonite was gradually incorporated into the chitosan solution and stirred continuously for two hours.
- Addition of STPP: The resulting mixture was combined with 100 mL of 5.0% (w/w) STPP solution and stirred for four hours to enhance colloidal stability.
- Filtration and Washing: The mixture was filtered and washed with distilled water until the pH reached 7 to remove residual acids and salts.
- Drying Process: The final product was dried in an oven at 60°C until a powdered form was obtained, making it suitable for further use.

This procedure was repeated for different time variations, as presented in Table I.

TABLE I. COMBINATOIN OF MIXING TIMES FOR BENTONITE AND CHITOSAN

Variation*	Mixing Time (h)		Total Mixing Time (h)
	Acetic Acid	STPP	
1	1	1	2
2	1	2	3
3	1	3	4
4	1	4	5
5	2	1	3
6	2	2	4
7	2	3	5
8	2	4	6

* The mixing times were based on previous studies [4-6, 11]

D. Characterization and Testing of Bentonite-Chitosan Mixture

The bentonite-chitosan mixture was subjected to a series of tests to evaluate its chemical composition, thermal stability, microstructural properties, plasticity, and permeability.

1) Chemical and Structural Characterization

- FTIR: Utilized to identify the functional groups and confirm the chemical interactions between bentonite and chitosan.
- TGA: Conducted to assess the thermal stability and decomposition behavior of the mixture.
- SEM with Energy Dispersive X-ray (SEM-EDX): Employed to examine the surface morphology and determine the elemental composition of the composite.

2) Geotechnical and Mechanical Testing

- LL and PL: Measured to evaluate the plasticity of the mixture.
- Permeability Test: Conducted using the falling head method under a compaction density of 16 kN/m^3 and a water content of 10%.

These conditions were selected to ensure consistency with previous studies, facilitating a direct comparison of the results.

III. RESULTS AND DISCUSSION

A. Bentonite-Chitosan Composite Characterization

1) Fourier-Transform Infrared Spectroscopy Analysis

The FTIR spectra of the bentonite-chitosan mixtures prepared with different mixing times, listed in Table I, reveal characteristic absorption bands associated with both the bentonite and chitosan functional groups, as depicted in Figure 3. A broad absorption band observed at 3,200-3,600 cm^{-1} corresponds to O-H and N-H stretching, indicating the presence of hydroxyl and amine groups from chitosan. Peaks at 1,650 cm^{-1} (amide I) and 1,560 cm^{-1} (amide II) confirm the successful incorporation of chitosan into the composite. The Si-O stretching bands at 1,000-1,200 cm^{-1} reflect the structural framework of bentonite. Longer mixing times result in sharper and more distinct absorption peaks, suggesting enhanced bonding interactions and improved composite uniformity. This observation aligns with previous studies highlighting the role of crosslinking agents in chitosan-bentonite composites: Authors in [6] demonstrated that glutaraldehyde crosslinking enhances the chitosan-bentonite interactions, leading to FTIR peaks at 3,360 cm^{-1} (O-H, N-H stretching) and 1,657 cm^{-1} (amide I). Similarly, authors in [18] found that epichlorohydrin-crosslinked composites exhibit strong bonding, characterized by O-H and N-H stretching at 3,444 cm-1 and amide peaks at 1,637 cm-1 and 1,590 cm^{-1}. These findings align with the improved structural stability observed in this study, where prolonged mixing times contribute to stronger chitosan-bentonite interactions. STPP plays a critical role in ionic crosslinking, introducing peaks for P=O and P–O–P groups (900-1,153 cm^{-1}), as noted in [19, 20]. Shifts in O-H/N-H bands following dye adsorption [21] further confirm its effectiveness in enhancing the adsorption properties.

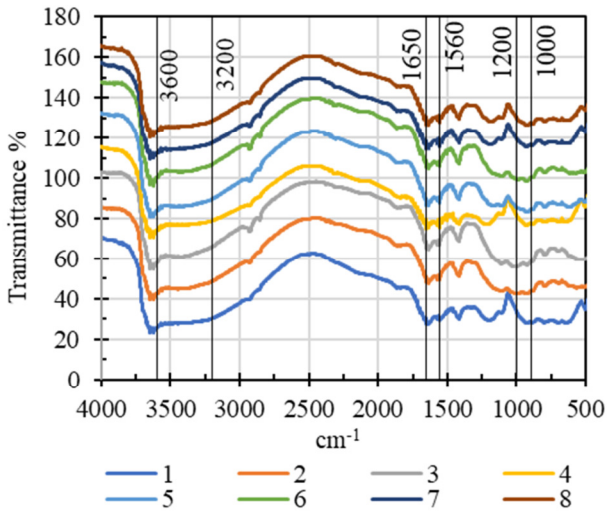

Fig. 3. FTIR spectra of bentonite-chitosan composites.

2) Thermogravimetric Analysis

The TGA results in Figure 4 illustrate the influence of the mixing time on the thermal behavior of the bentonite-chitosan composites (Samples 1, 4, 5, and 8). The weight loss patterns are categorized into three district stages:

a) Initial Stage (25–200°C):

- Pure bentonite exhibits the highest initial weight loss, primarily due to its high moisture content.
- Chitosan-bentonite composites present reduced weight loss in this range, indicating that chitosan incorporation lowers the moisture adsorption by modifying the material's hydrophilic properties.

b) Decomposition Stage (200–400°C):

- The decomposition of organic components is more pronounced in chitosan-containing composites.
- Sample 8, prepared with extended acetic acid and STPP mixing, exhibits the highest thermal stability, suggesting stronger chitosan-bentonite interactions and improved polymer crosslinking.

c) Final Stage (400–600°C):

- Minimal weight loss is observed, particularly in Sample 8, highlighting the stabilizing effect of optimized mixing conditions.
- This suggests that longer mixing durations enhance composite structural integrity by reinforcing crosslinking networks between chitosan and bentonite.

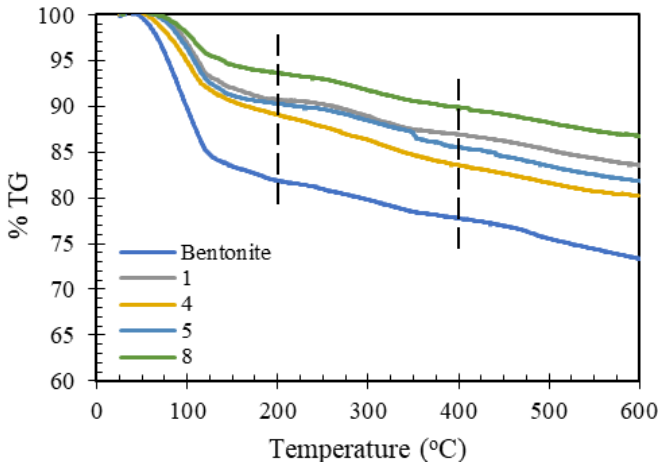

Fig. 4. TGA curves of bentonite and bentonite-chitosan composites.

The observed thermal stability trends align with prior research on crosslinked chitosan-bentonite composites. Specifically, authors in [15] reported enhanced thermal stability in glutaraldehyde-crosslinked chitosan composites, where bentonite integration significantly reduced the mass loss at higher temperatures. Similarly, in [18], distinct weight-loss stages were observed in epichlorohydrin-crosslinked chitosan-bentonite composites, highlighting the role of crosslinking in improving the thermal resistance. Authors in [16] noted improved crystallinity and thermal behavior in CTAB-bentonite-chitosan films, with significant reductions in weight loss below 150°C and between 200–350°C. Additionally, authors in [19] reported moisture-related weight loss at 90°C and decomposition at 285°C in tripolyphosphate-crosslinked chitosan hydrogels, emphasizing the role of crosslinkers in

stabilizing composites. In [20], an enhanced stability in ion-imprinted magnetic nanocomposite bentonite was observed, indicating a weight loss below 100°C and a structural degradation between 200–800°C. Finally, authors in [21] further identified the synergistic effects in Russula delica/bentonite/tripolyphosphate composites, enhancing the thermal stability during decomposition stages at 260–310°C and 750–800°C.

3) Scanning Electron Microscopy with Energy Dispersive X-ray Analysis

The SEM images of the bentonite-chitosan composites for Samples 1, 4, 5, and 8 reveal progressive morphological changes in cluster structure and particle distribution, influenced by the mixing conditions, as portrayed in Figure 5. Sample 1 displays loosely packed clusters with irregular shapes and larger voids, suggesting a weak interaction between bentonite and chitosan due to shorter mixing times. In Sample 4, the clusters are more compact with reduced void spaces, indicating an improved dispersion and partial integration of chitosan into the bentonite matrix. Sample 5 presents tightly packed clusters with smaller voids, reflecting an enhanced interaction and better chitosan dispersion, likely due to the extended acetic acid mixing time. Sample 8 demonstrates the most cohesive and compact clusters with minimal voids and uniform particle distribution, indicating an optimal integration of chitosan into the bentonite structure, achieved through the longest mixing times for both acetic acid and STPP. These observations confirm that longer mixing durations enhance composite uniformity, likely improving performance in clay liner applications by reducing the permeability and increasing the mechanical stability.

The EDX data in Table II present the elemental composition of the bentonite and bentonite-chitosan composites prepared under different mixing conditions (Sample 1, 4, 5, and 8). Pure bentonite is composed primarily of oxygen (49.7 wt%) and silicon (11.0 wt%), reflecting its clay-based structure. Minimal carbon (30.4 wt%) indicates the absence of organic components. In Sample 1, with 1-hour mixing with both acetic acid and STPP, a slight carbon increase is observed (31.6 wt%), suggesting a limited chitosan integration. No phosphorus is detected, indicating insufficient STPP crosslinking. In Sample 4, with 1-hour acetic acid and 4-hour STPP mixing, a higher carbon content is presented (42.4 wt%), confirming stronger chitosan presence, and detectable phosphorus, demonstrating enhanced ionic crosslinking between chitosan and STPP. In Sample 5, with 2-hour acetic acid and 1-hour STPP mixing, yield moderate carbon (38.4 wt%) and undetectable phosphorus are noted, indicating less effective crosslinking. Sample 8, with 2-hour acetic acid and 4-hour STPP mixing, balances carbon (32.0 wt%) and phosphorus, reflecting optimal interactions. These results highlight that longer STPP mixing times, as in Variants 4 and 8, significantly improve crosslinking and composite stability, while the extended acetic acid mixing enhances the chitosan distribution.

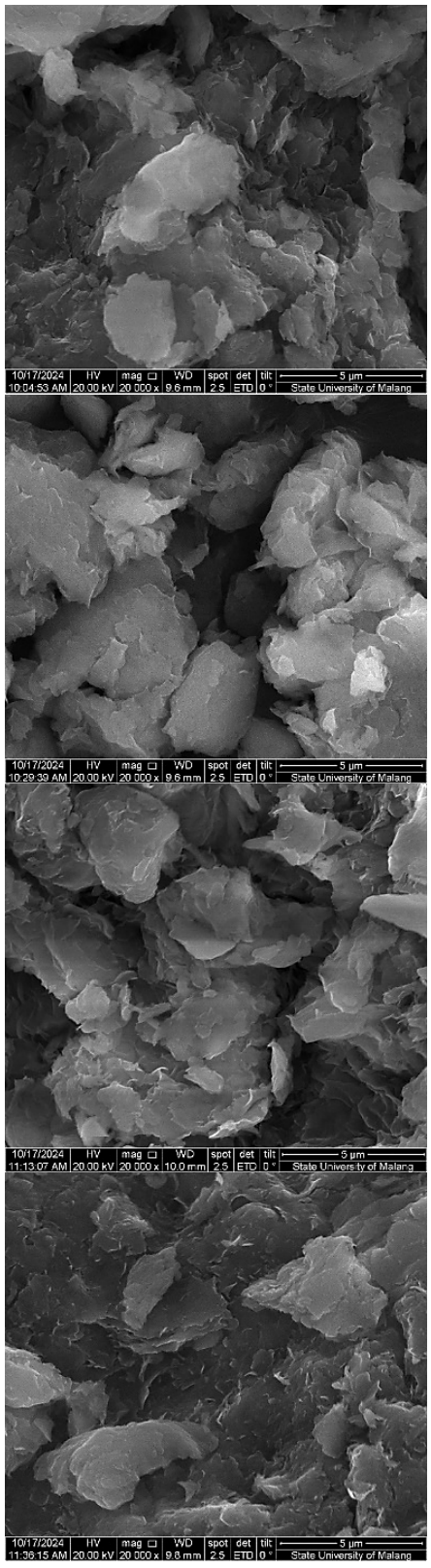

Fig. 5. SEM images of bentonite-chitosan composites: (a) variant 1, (b) variant 4, (c) variant 5, and (d) variant 8.

TABLE II. EDX DATA OF BENTONITE AND BENTONITE CHITOSAN COMPOSITE

Element	Bentonite	Bentonite-Chitosan			
		1	4	5	8
C K	30.4	31.6	42.4	38.4	32.0
O K	49.7	49.1	44.1	44.3	49.4
Na K	1.0	1.6	1.2	1.0	1.6
Mg K	0.4	0.3	0.2	0.2	0.3
Al K	4.5	4.0	2.9	3.0	4.0
Si K	11.0	9.6	7.1	9.1	9.6
Ca K	0.6	0.6	0.4	0.6	0.5
Ti K					0.2

B. Plasticity Characteristics

The plasticity characteristics of bentonite-chitosan composites were evaluated by analyzing the LL and PI across different mixing times, as shown in Figure 6. Pure bentonite (Sample 0) exhibited an LL of approximately 370% and a PI of about 330%, serving as a baseline. The addition of chitosan increased both LL and PI across all samples, primarily due to chitosan's ability to enhance water retention and its electrostatic interactions with bentonite, which improve the soil plasticity.

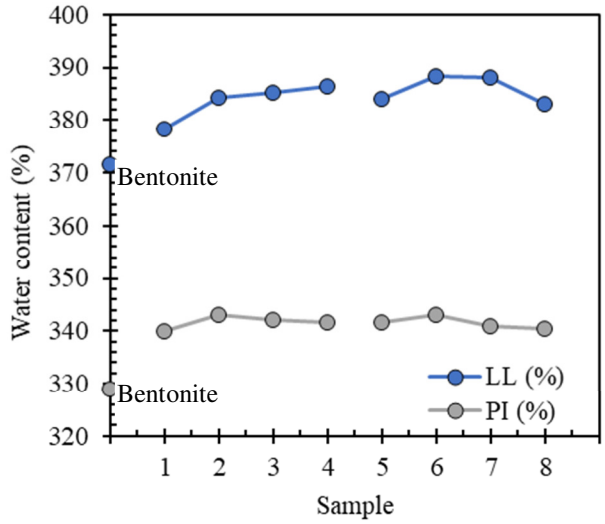

Fig. 6. LL and PI of bentonite-chitosan composites.

The samples prepared with a longer acetic acid mixing time (Samples 5–8) exhibited slightly higher LL and PI values than those mixed for only one hour (Samples 1–4), indicating that the prolonged acetic acid mixing improves the chitosan dissolution and distribution within the bentonite matrix. Similarly, extended STPP mixing further increased LL, likely due to enhanced crosslinking between chitosan and bentonite, although its effect on PI was less pronounced. These results highlight the importance of optimizing both acetic acid and STPP mixing times to achieve improved plasticity and water retention in bentonite-chitosan composites.

C. Permeability Performance

The permeability performance of bentonite-chitosan composites was assessed using the falling head method, as illustrated in Figure 7. Pure bentonite (Sample 0) exhibited a a permeability coefficient of approximately 1×10^{-12} m/s, which was closely matched by Sample 8, prepared with the longest acetic acid and STPP mixing times, confirming the effectiveness of optimized mixing. The addition of chitosan significantly reduced the permeability in all samples, with the lowest values being observed in Samples 7 and 8, indicating that prolonged mixing enhances composite impermeability. The samples with a longer acetic acid mixing duration (Samples 5–8) exhibited consistently lower permeability than those mixed for a shorter time (Samples 1–4), suggesting that extended acetic acid mixing improves the chitosan dispersion within the bentonite matrix. Likewise, longer STPP mixing times, particularly in Samples 4 and 8, contributed to stronger crosslinking, further reducing permeability. These findings confirm that optimizing both acetic acid and STPP mixing times enhances the chitosan integration, crosslinking, and impermeability, making the composites highly suitable for clay liner applications.

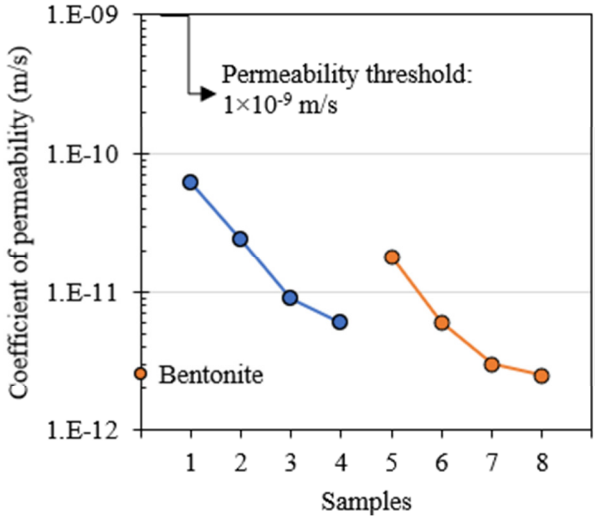

Fig. 7. Permeability coefficient of bentonite and bentonite-chitosan composites.

The findings align with other characterization results, reinforcing the impact of optimized mixing conditions on composite performance. The FTIR analysis indicates stronger chemical interactions in Samples 7 and 8, as evidenced by the more pronounced functional group peaks, while TGA results reveal an improved thermal stability, reflecting enhanced structural integrity. The SEM analysis further supports these observations, showing that Samples 7 and 8 possess more compact and cohesive clusters with minimal void spaces, effectively reducing permeability. Additionally, the higher LL and PI values in these samples suggest better water retention and plasticity, which contribute to improved void sealing and resistance to water flow.

Although pure bentonite exhibits similarly low permeability to Sample 8, it lacks the structural integrity provided by chitosan. Without chitosan, the bonds between bentonite particles are weaker, and when mixed with 90% sand (represented by the green cross marker in Figure 8), the permeability increases significantly, failing to meet the

required threshold of 1×10^{-9} m/s [5]. This highlights the inability of pure bentonite to effectively seal sand pores, despite its initially low permeability. This contrast underscores the crucial role of chitosan in reinforcing structural integrity and ensuring consistent performance.

The bentonite-chitosan composites studied here consistently maintain low permeability, as indicated by the red data points in Figure 8. These results emphasize the significant role of chitosan in reducing permeability by enhancing interparticle bonding and controlling the swelling behavior. In contrast, previous studies on Chitosan-Betonite-Sand (CBS) composites with high sand content (70%–90%) [5, 11] demonstrated that the sand addition had a minimal impact on permeability, as CBS composites still retained values below the threshold of 1×10^{-9} m/s. This finding highlights the stabilizing effect of chitosan, which enables CBS composites to maintain low permeability even at high sand fractions, further reinforcing its suitability for sustainable clay liner applications.

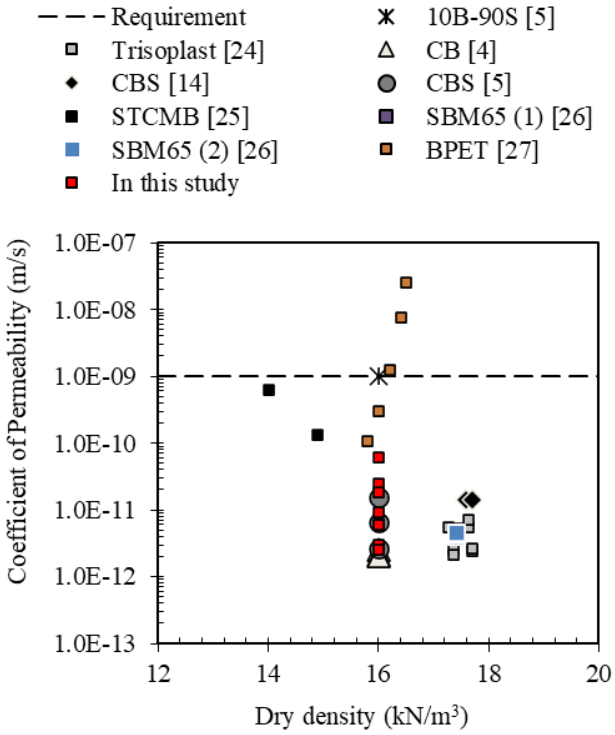

Fig. 8. Comparison of permeability coefficients for bentonite-chitosan composites and other bentonite-polymer-based materials.

In comparison, other materials, such as Trisoplast (grey squares) [23], STCMB (black squares) [24], SBM65 (blue squares) [25], and BPET (green squares) [26], also achieve compliance with the regulatory standards but rely on synthetic polymers or chemical modifications [25, 26]. In contrast, this study's bentonite-chitosan composite, which is free of sand and synthetic additives, matches or even surpasses these materials in permeability performance. This highlights the effectiveness of natural polymer integration in bentonite, demonstrating that chitosan can enhance the barrier properties without the need for extensive chemical modifications. These findings validate the potential of bentonite-chitosan composites as an environmentally friendly and high-performing alternative, particularly for applications requiring low permeability and minimal chemical additives, making them a sustainable option for clay liner applications.

D. Optimal Mixing Time and Future Research Direction

Based on the analysis of permeability, FTIR, TGA, SEM, LL, and PI, Sample 8, with a total mixing time of 6 hours (2 hours with acetic acid and 4 hours with STPP), demonstrates the most optimal properties. However, this extended mixing duration may not be practical for large-scale applications due to its high time and energy requirements. A more feasible alternative is Sample 6, which requires a total mixing time of 4 hours (2 hours with acetic acid and 2 hours with STPP). This sample achieves low permeability and good structural integrity while significantly reducing the processing time compared to Sample 8. The shorter mixing duration still allows for sufficient chitosan dissolution and crosslinking, making it more suitable for field applications. The structural improvements align with the findings in [8], where it was demonstrated that the incorporation of montmorillonite into the chitosan systems enhances the porosity and mechanical integrity. Similarly, authors in [7] highlighted that optimized preparation conditions improve the intercalation and interaction between chitosan and clay minerals, which are critical for achieving the desired composite performance. Additionally, authors in [27] emphasized the importance of structural reinforcement in landfill covers, highlighting the potential of fiber-based composites in enhancing mechanical stability. Authors in [28] demonstrated that coupling agents, such as L-leucine and stearic acid, significantly improve the thermal and mechanical properties of polymer-clay composites, supporting the observed benefits of optimized preparation conditions. To validate this proposal, further research should be conducted to assess the long-term durability of composites prepared with shorter mixing times, particularly under field conditions. Additional studies on scaling up the mixing process, performance in sand-bentonite mixtures, and alternative mixing methods could provide further insights into the practical implementation of bentonite-chitosan composites.

IV. CONCLUSION

This study explored the impact of mixing time on the properties and performance of bentonite-chitosan composites, with a focus on their potential as clay liners. The findings underscore the novelty of the research by demonstrating that extended mixing times significantly enhance the integration of chitosan into the bentonite matrix, resulting in notable improvements in permeability reduction, plasticity, and thermal stability. The Fourier-Transform Infrared Spectroscopy (FTIR), Thermogravimetric Analysis (TGA), and Scanning Electron Microscopy (SEM) revealed that longer mixing durations lead to composites with stronger chemical interactions, improved thermal resistance, and more cohesive, compact structures. Notably, the optimized mixing time of 6 hours (Sample 8) achieved the lowest permeability, which was comparable to pure bentonite, while overcoming its structural integrity limitations when mixed with sand.

The present study offers significant contributions by highlighting the vital role of chitosan in enhancing interparticle bonding and sealing properties, particularly in sand-bentonite composites. Compared to previous studies, the incorporation of chitosan presents a natural and environmentally friendly alternative to synthetic polymers, offering similar or superior performance in terms of permeability and structural stability. Furthermore, this research provides valuable insights into balancing performance and efficiency, with Sample 6 (4 hours of mixing) presenting a practical alternative for field applications. By investigating the influence of mixing time on the structural and functional properties of bentonite-chitosan composites, this study advances the understanding of composite optimization for clay liner applications. Future research should focus on evaluating the long-term durability of these composites under real-world conditions, scaling up the mixing process, and assessing their performance in sand-bentonite mixtures to further confirm their practicality and sustainability in broader applications.

ACKNOWLEDGMENT

This research was supported by the Competitive Research Program-Fundamental Research Scheme under contract number 1374.114/UN8.2/PG/2024 and funded by the University of Lambung Mangkurat.

REFERENCES

[1] L. Zhao *et al.*, "Berberine-Loaded Carboxylmethyl Chitosan Nanoparticles Ameliorate DSS-Induced Colitis and Remodel Gut Microbiota in Mice," *Frontiers in Pharmacology*, vol. 12, Apr. 2021, https://doi.org/10.3389/fphar.2021.644387.

[2] N. Hataf, P. Ghadir, and N. Ranjbar, "Investigation of soil stabilization using chitosan biopolymer," *Journal of Cleaner Production*, vol. 170, pp. 1493–1500, Jan. 2018, https://doi.org/10.1016/j.jclepro.2017.09.256.

[3] Y. Kulshreshtha *et al.*, "Biological Stabilisers in Earthen Construction: A Mechanistic Understanding of their Response to Water-Ingress," *Construction Technologies and Architecture*, vol. 1, pp. 529–539, 2022, https://doi.org/10.4028/www.scientific.net/CTA.1.529.

[4] T. Hidayat and Y. F. Arifin, "The Potential of Bentonite and Chitosan Mixtures as Clay Liner Base Material," *IOP Conference Series: Earth and Environmental Science*, vol. 1184, no. 1, May 2023, Art. no. 012011, https://doi.org/10.1088/1755-1315/1184/1/012011.

[5] E. Erwansyah and Y. F. Arifin, "Chitosan-enhanced bentonite-sand mixture as a clay liner," in *Proccedings of the 4th International Conference on Green Civil and Environmental Engineering*, Bali, Indonesia, Mar. 2024, https://doi.org/10.1063/5.0204897.

[6] R. Aguilar *et al.*, "The potential use of chitosan as a biopolymer additive for enhanced mechanical properties and water resistance of earthen construction," *Construction and Building Materials*, vol. 114, pp. 625–637, Jul. 2016, https://doi.org/10.1016/j.conbuildmat.2016.03.218.

[7] M. D. Alba, A. Cota, F. J. Osuna, E. Pavón, A. C. Perdigón, and F. Raffin, "Bionanocomposites based on chitosan intercalation in designed swelling high-charged micas," *Scientific Reports*, vol. 9, no. 1, Jul. 2019, Art. no. 10265, https://doi.org/10.1038/s41598-019-46495-z.

[8] B. F. F. dos Santos *et al.*, "Synthesis and Preparation of Chitosan/Clay Microspheres: Effect of Process Parameters and Clay Type," *Materials*, vol. 11, no. 12, Dec. 2018, Art. no. 2523, https://doi.org/10.3390/ma11122523.

[9] Y. F. Arifin, M. Arsyad, A. A. Pangestu, and D. Pratama, "The Permeability and Shear Strength of Compacted Claystone-Bentonite Mixtures," *GEOMATE Journal*, vol. 21, no. 84, pp. 48–61, Nov. 2021.

[10] S. S. Agus and Y. F. Arifin, "Compacted Polymer-Enhanced Bentonite-Sand Mixture– Behaviour and Potential Applications," in *20th SEAGC-3rd AGSEA Conference in conjunction with 22nd Annual Indonesia National Conference on Geotechnical Engineering*, Jakarta, Indonesia, Nov. 2018, pp. 415–420.

[11] M. S. Hosney and R. K. Rowe, "Performance of polymer-enhanced bentonite–sand mixture for covering arsenic-rich gold mine tailings for up to 4 years," *Canadian Geotechnical Journal*, vol. 54, no. 4, pp. 588–599, Apr. 2017, https://doi.org/10.1139/cgj-2016-0375.

[12] C. Zhang, X. Wei, C. Zhang, Y. Li, Y. Sheng, and S. Peng, "Study on Preparation of Polymer-Modified Bentonite and Sand Mixtures Based on Osmotic Pressure Principle," *Materials*, vol. 15, no. 10, Jan. 2022, Art.no. 3643, https://doi.org/10.3390/ma15103643.

[13] N. Salsabila, Y. Arifin, and A. Pratiwi, "Compaction Parameters of a Chitosan-Bentonite-Sand Mixture," presented at the *Proceedings of the 1st International Conference on Environmental Science, Development, and Management, ICESDM 2023*, 2 November 2023, Banjarmasin, South Kalimantan, Indonesia, Aug. 2024.

[14] Q. U. Ain, U. Rasheed, K. Liu, Z. Chen, and Z. Tong, "Synthesis of 2-amino-terephthalic acid crosslinked chitosan/bentonite hydrogel; an efficient adsorbent for anionic dyes and laccase," *International Journal of Biological Macromolecules*, vol. 258, Feb. 2024, Art. no. 128865, https://doi.org/10.1016/j.ijbiomac.2023.128865.

[15] R. El Kaim Billah *et al.*, "A novel glutaraldehyde cross-linked chitosan@acid-activated bentonite composite for effectiv Pb (II) and Cr (VI) adsorption: Experimental and theoretical studies," *Separation and Purification Technology*, vol. 334, Apr. 2024, Art. no. 126094, https://doi.org/10.1016/j.seppur.2023.126094.

[16] M. Gülpınar, F. Tomul, Y. Arslan, and H. N. Tran, "Chitosan-based film incorporated with silver-loaded organo-bentonite or organo-bentonite: Synthesis and characterization for potential food packaging material," *International Journal of Biological Macromolecules*, vol. 274, Aug. 2024, Art. no. 133197, https://doi.org/10.1016/j.ijbiomac.2024.133197.

[17] N. Jahan, M. A. Al Fahad, P. C. Shanto, H. Kim, B.-T. Lee, and S. H. Bae, "Development of self-gelling powder combining chitosan/ bentonite nanoclay/ sodium polyacrylate for rapid hemostasis: *In vitro* and *in vivo* study," *International Journal of Biological Macromolecules*, vol. 291, Feb. 2025, Art. no. 139123, https://doi.org/10.1016/j.ijbiomac.2024.139123.

[18] A. Benhouria, H. Zaghouane-Boudiaf, R. Bourzami, F. Djerboua, B. H. Hameed, and M. Boutahala, "Cross-linked chitosan-epichlorohydrin/bentonite composite for reactive orange 16 dye removal: Experimental study and molecular dynamic simulation," *International Journal of Biological Macromolecules*, vol. 242, Jul. 2023, Art. no. 124786, https://doi.org/10.1016/j.ijbiomac.2023.124786.

[19] N. A. Medellín-Castillo *et al.*, "Formaldehyde and tripolyphosphate crosslinked chitosan hydrogels: Synthesis, characterization and modeling," *International Journal of Biological Macromolecules*, vol. 183, pp. 2293–2304, Jul. 2021, https://doi.org/10.1016/j.ijbiomac.2021.06.020.

[20] C. Wang *et al.*, "Synthesis of environmental-friendly ion-imprinted magnetic nanocomposite bentonite for selective recovery of aqueous Sc(III)," *Journal of Colloid and Interface Science*, vol. 630, pp. 738–750, Jan. 2023, https://doi.org/10.1016/j.jcis.2022.10.161.

[21] A. Yildirim and H. Acay, "Methylene blue and malachite green dyes adsorption onto russula delica/bentonite/tripolyphosphate," *Heliyon*, vol. 11, no. 1, Jan. 2025, https://doi.org/10.1016/j.heliyon.2024.e41250.

[22] J. Yang, B. Huang, and M. Lin, "Adsorption of Hexavalent Chromium from Aqueous Solution by a Chitosan/Bentonite Composite: Isotherm, Kinetics, and Thermodynamics Studies," *Journal of Chemical & Engineering Data*, vol. 65, no. 5, pp. 2751–2763, May 2020, https://doi.org/10.1021/acs.jced.0c00085.

[23] T. Schanz, S. S. Agus, and G. Tscheschlok, "Hydraulisch-mechanische Eigenschaften einer polymerverbesserten Sand-Bentonit-Mischung beim Einsatz im Deponiebau," *Geotechnik*, vol. 27, no. 4, pp. 344–355, 2004.

[24] H. Ni, R.-D. Fan, K. R. Reddy, and Y.-J. Du, "Containment of phenol-impacted groundwater by vertical cutoff wall with backfill consisting of sand and bentonite modified with hydrophobic and hydrophilic polymers," *Journal of Hazardous Materials*, vol. 461, Jan. 2024, Art. no. 132627, https://doi.org/10.1016/j.jhazmat.2023.132627.

[25] M. S. Biju and D. N. Arnepalli, "Effect of biopolymers on permeability of sand-bentonite mixtures," *Journal of Rock Mechanics and*

Geotechnical Engineering, vol. 12, no. 5, pp. 1093–1102, Oct. 2020, https://doi.org/10.1016/j.jrmge.2020.02.004.

[26] A. Chandra and S. Siddiqua, "Sustainable utilization of chemically depolymerized polyethylene terephthalate (PET) waste to enhance sand-bentonite clay liners," *Waste Management*, vol. 166, pp. 346–359, Jul. 2023, https://doi.org/10.1016/j.wasman.2023.04.030.

[27] M. Jamei, A. Mabrouk, and Y. Alassaf, "Influence of Deflection Deformations on the Sustainability of the Landfill Cover: Analysis and Recommendations," *Engineering, Technology & Applied Science Research*, vol. 14, no. 3, pp. 14387–14394, Jun. 2024, https://doi.org/10.48084/etasr.7364.

[28] N. Mohammedi, F. Zoukrami, and N. Haddaoui, "Preparation of Polypropylene/Bentonite Composites of Enhanced Thermal and Mechanical Properties using L-leucine and Stearic Acid as Coupling Agents," *Engineering, Technology & Applied Science Research*, vol. 11, no. 3, pp. 7207–7216, Jun. 2021, https://doi.org/10.48084/etasr.4148.